Int. J. Electrochem. Sci., 10 **(2015)** 4116 - 4128

International Journal of
ELECTROCHEMICAL
SCIENCE
www.electrochemsci.org

Corrosion Behavior of Super Duplex Stainless Steel S32750 in White Liquor

Hao Feng[1], *Huabing Li*[1,*], *Shucai Zhang*[1], *Qi Wang*[1], *Zhouhua Jiang*[1], *Guoping Li*[2], *Wei Zhang*[2], *Guangwei Fan*[2]

[1] School of Materials and Metallurgy, Northeastern University, Shenyang 110819, China
[2] Technology Center of Taiyuan Iron and Steel Croup Co. Ltd., Taiyuan 030001, China
[*]E-mail: lihb@smm.neu.edu.cn

Received: 7 February 2015 / *Accepted:* 9 March 2015 / *Published:* 23 March 2015

The effect of temperature on the corrosion behavior of super duplex stainless steel S32750 in white liquor was evaluated using potentiodynamic polarization, potentiostatic polarization, electrochemical impedance spectroscopy and Mott-Schottky analysis. The corrosion current density and steady state current density increases, and the induction period of the pits is shortened with increasing temperature, indicating that the corrosion process is accelerated and protective ability of the passive film decreases at higher temperatures. The pit occurred around the $MgO \cdot Al_2O_3$ composite inclusion with residual MnS, indicating the preferential partial dissolution of MnS. EIS results reveal that the protection of the passive film is predominantly attributed to the barrier film, and the passive film becomes more porous and less protective at higher temperatures. The passive film presents a bilayer structure and behaves as n-type and p-type, respectively and it becomes more defective at higher temperatures. The donor and acceptor densities increase and the space charge layer thickness decreases with temperature. Therefore, the passive films become more defective, resulting in decreased protective abilities of the passive films.

Keywords: Super Duplex Stainless Steel, White Liquor, Corrosion Behavior, Temperature, Passive Films

1. INTRODUCTION

Pulp and paper industry is closely related to economic and human civilization development and 90% of pulps are produced using the kraft pulping process. In this process, white liquor is added and black liquor extracted in several locations or phases of the cooking process[1]. White liquor contains the highest concentration of sodium hydroxide (NaOH) and sodium sulphide (Na_2S), which is considered to be the most aggressive of all pulping liquors[2,3]. Sulphide exists mainly in hydrated form (HS^-), but also in the forms of sulphide (S^{2-}) and polysulphides (S_n^{2-}, n = 2, 3, 4, 5…). Minor

quantities of higher valency sulphur in the form of thiosulphate, sulphite and sulphate are also believed to be exist[2,4,5]. The presence of aggressive ions results in serve corrosion problems, including local corrosion, uniform corrosion, erosion-corrosion, and stress corrosion cracking[6].

Pulp and paper industry has undergone rapid changes during the last decade, among which duplex steel is the biggest material breakthrough, due to its excellent corrosion resistance, high mechanical strength and the thickness reductions this enables[7]. Carbon steel was used for kraft digesters previously, but it is susceptible to uniform corrosion and stress corrosion cracking (SCC), and corrode severely in sulphide-containing caustic solutions[6]. Austenitic stainless steels, often clad on carbon steel, was used for digesters and pulp storage towers to reduce maintenance costs resulting from corrosion[8]. However, there is occasionally poor adhesion between the cladding and the substrate and three or maybe four different types of welding consumables lead to the complex welding procedures[9]. In addition, Type 304L and 316L stainless steel can experience rapid corrosion thinning resulting in exposure of the carbon steel substrate[6]. The use of a solid duplex (ferritic-austenitic) stainless steel provides the advantages of both reduced material requirements for the initial investment and low maintenance. It is reported that the total investment of a solid duplex stainless steel tower using UNS S32304 might yield cost savings of 8% compared to a tower of carbon steel lined with austenitic stainless steel[8]. The higher alloyed super duplex S32750 with higher mechanical strength exhibits excellent corrosion resistance in harsh environment, which is an ideal alternative material for pulp and paper industry in order to prolong service life.

In recent years, several references on the corrosion behavior for carbon steel, austenitic and duplex stainless steel in sulphide-containing caustic solutions have been published[1,2,4,5,10]. Wensley reported that sulfide and thiosulfate ions hindered the passivation of mild steel, while sulfite and sulfate ions had no effect, and polysulfide ions controlled the corrosion potential[10]. Betova reported that sulphide prevents the formation of a stable passive film, most probably via adsorption on the surface. As a result, the dominant mechanism of corrosion in sulphide-containing environments becomes similar to active dissolution, which could lead to significant material losses [5]. Bhattacharya revealed that the corrosion rates of duplex stainless steels increase with temperature and sulphide addition to caustic environments[2]. However, there is scarcely any information on the corrosion behavior and electrical properties of S32750 in white liquor can be found.

In the present work, the effect of temperature on corrosion behavior of super duplex stainless steel S32750 in white liquor was investigated. In addition, duplex stainless steel S32205 currently used in pulp and paper industry was used to compare the corrosion resistance with S32750 in white liquor. The electrochemical behavior, passivation kinetics and semiconducting properties were performed at different temperatures (40, 60 and 80℃) to reveal the effect of temperature on corrosion behavior in simulating pulp and paper industry.

2. EXPERIMENTAL

2.1 Material and test preparation

The steels S32750 and S32205 used in this study are supplied by TISCO and the chemical composition are shown in Table 1. The steels were made in electric arc furnace, followed by argon

oxygen decarburization (AOD) refining and continuous casting, and then hot rolled into 6 mm thick plate. The hot rolled steels were finally solution treated at 1080 ℃ for 1 h and quenched to room temperature. The sample was etched using 30 wt.% KOH and then examined by a Carl Zeiss Ultra Plus Field Emission scanning electron microscope (SEM). The microstructure of S32750 consists of grains of ferritic and austenitic, and the volume fractions of both phases were close to 50 %, as shown in Fig. 1. The specimens of 10.1 mm×10.1 mm were cut from the solution treated hot rolled plate and polished with SiC papers from 200 to 2000 grits. The passivation treatment of the specimens was performed in 20-30 wt% nitric acid solution at 50℃ for 1 h to avoid crevice corrosion at high temperature. The working surface of electrodes exposed to the solution was 1 cm^2 and other unexposed area was mounted in an epoxy resin with the wire for electrical connection. The electrochemical tests were performed in synthetic white liquor (3.75 M NaOH + 0.64 M Na_2S solution), which was prepared using 150 g/L of NaOH and 153.8 g/L of reagent grade $Na_2S·9H_2O$[2].

Table 1. Chemical composition of steels used in the present study (wt%)

Steel	C	Cr	Ni	Mo	N	Si	Mn	P	S	Cu	Fe
S32750	0.018	25.02	7.02	3.94	0.28	0.70	0.93	0.029	0.0005	0.07	Bal.
S32205	0.021	22.27	5.25	3.14	0.17	0.51	1.05	0.028	0.001	-	Bal.

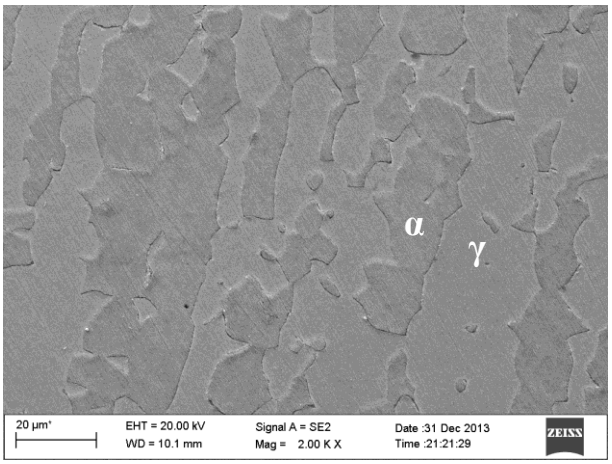

Figure 1. SEM image of super duplex stainless steel S32750

2.2 Electrochemical measurements

Gamry Reference 600 potentiostats were used for electrochemical tests with a standard three-electrode system, which consisted of a platinum foil counter electrode, a saturated calomel reference electrode and specimen as working electrode. Electrochemical measurements were performed at 40, 60 and 80 ℃ using a HH-601 super thermostatic water bath to investigate the effect of temperature on the corrosion behavior of S32750 in white liquor. Concerning the presence of oxygen in paper industry, deoxygenating was not conducted to keep consistent with service environments.

Potentiodynamic anodic polarization measurements were performed at a sweep rate of 1 mV/s from -0.2 V below OCP until the current density reached 10 mA/cm^2. Potentiostatic polarization measurements were conducted to obtain the current transient at a constant applied potential. Prior to measurement, the working electrode was polarized to -1.0 V_{SCE} for 600 s to remove the passive film formed in air. Then the chosen potential (-0.4 V_{SCE}) was applied for 15000 s and the potentiostatic current density was recorded. The passive film was formed under the potential of -0.4 V_{SCE} for 1 h for electrochemical impedance spectroscopy (EIS) and capacitance measurements. EIS measurements were carried out with voltage amplitude of 10 mV in the frequency ranging from 100 kHz to 0.01 Hz, and fitting was performed with ZSimpWin software. The capacitance measurements of passive film were carried out at a fixed frequency 1000 Hz at 5 mV amplitude voltage initiated at -0.4 to -1.4 V_{SCE} in the cathodic direction by 40 mV steps. Microscopic examination was also performed by using SEM and energy dispersive spectrometer (EDS) after potentiostatic polarization measurement.

3. RESULTS AND DISCUSSION

3.1 Potentiodynamic polarization results

The potentiodynamic polarization curves of S32750 and S32205 in white liquor in the temperature range from 40 to 80 ^{0}C are shown in Fig. 2. The temperature dependence of cathodic reaction was observed due to the cathodic current densities increasing with temperature. And the kinetics of anodic dissolution of the steel is also favored with increasing temperature owing to anodic current densities increasing at higher temperature. From the potentiodynamic curves, the values of tafel slopes (β_a, β_c), corrosion potential (E_{corr}), corrosion current density (i_{corr}) and critical current density (i_{crit}) were obtained and listed in Table 2.

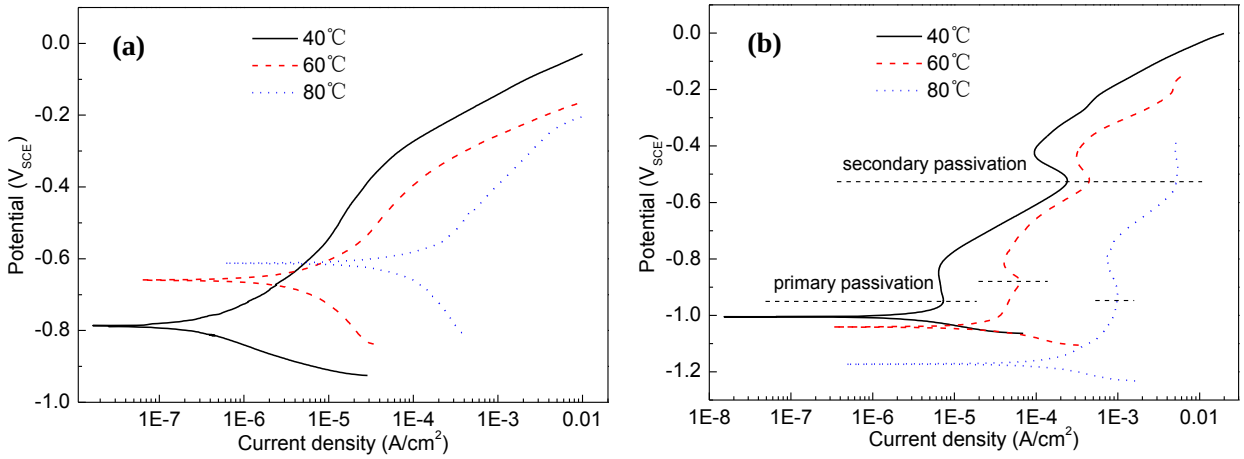

Figure 2. Potentiodynamic polarization curves of S32750 (a) and S32205 (b) in white liquor at different temperatures

The values of β_a, β_c and i_{corr} of both steels increased with temperature, indicating the acceleration of corrosion rates at higher temperatures. The increasing of E_{corr} of S32750 with temperature is related to the increment of cathodic current density[11]. However, E_{corr} of S32205 decreases with increasing temperature, which makes it difficult to attain passivation in white liquor. In addition, the values of i_{crit} of S32205 increased with temperature ranging from 40 to 80 ^{0}C.

Table 2. Electrochemical parameters of potentiodynamic polarization at different temperatures

Steel	Temperature(℃)	E_{corr}(V$_{SCE}$)	i_{corr}(A·cm^{-2})	β_a(V)	β_c(V)	i_{crit}(A·cm^{-2})
S32750	40	-0.79	2.99×10^{-7}	0.121	0.087	Already passivated
	60	-0.66	9.50×10^{-6}	0.228	0.361	Already passivated
	80	-0.61	8.48×10^{-5}	0.199	0.558	Already passivated
S32205	40	-1.01	1.42×10^{-6}	0.065	0.035	7.33×10^{-6}
	60	-1.04	2.61×10^{-5}	0.173	0.064	6.40×10^{-5}
	80	-1.17	1.39×10^{-4}	0.249	0.094	9.96×10^{-4}

It is noteworthy that on the anodic branch of the curves, the absence of active current peak or Flade potential of S32750 in Fig. 2(a) confirms the passive films previously formed on S32750 in air kept passivity in white liquor[2,12]. However, S32205 in Fig. 2(b) behaved primary and secondary active-passive transition zones, which is consistent with other research[2]. The current peak before primary passivation is associated with the combined effect of Fe and Ni behavior in this potential range. Furthermore, Fe, Cr and Ni contributed to the primary passivation of S32205[2]. With the increment of applied potential, the second current peak at -0.5 V$_{SCE}$ was consider to correspond to Eq. (1).[13,14]

$$Cr_2O_3 + 5H_2O = 2CrO_4^{2-} + 10H^+ + 6e \quad (1)$$

Beyond the secondary active-passive transition, the secondary passivation observed was owing to the passive range for the iron and the continuing passivation of nickel[2]. In the present study, passivation at 80 ^{0}C cannot be obviously observed, which is in agreement with our previous work on S32750 in artificial sea water[14]. It was reported that presence of Cr^{6+} ion may contribute to the stability of passive films[15]. And the absence of passivation may be related to the decreasing concentration of dissolved oxygen and oxygen reduction rate and decreasing of the pH values in some localized micro-regions[16], which prevents the formation Cr^{6+}.

The results represent that the anodic dissolution of both the steels is accelerated and the protective properties of passive film become more defective at higher temperature. The main factor inducing the decrement of the protective properties of the films formed at higher temperatures is the changes of passive films composition with increasing temperature[17]. Additionally, the increment of porosity is another change of passive film properties with increasing temperature. Similar results have been reported by several authors[18-20].

Truman reported that the better corrosion resistance of duplex stainless steels can be attributed to the higher chromium content and controlled, intermediate nickel content in the steel[21]. According to the study by Bhattacharya, Fe with Cr and Ni helps to raise the corrosion potential and lower critical current density of duplex stainless steels in white liquor, thus improving corrosion resistance. However, the polarization curve of Mo did not show any active-passive or passivity. And the high dissolution rate of Mo in the form of MoO_4^{2-} or molybdate ion did not provide any protection against corrosion, indicating the detrimental effect of Mo on corrosion resistance of the steel[2]. In addition, the importance of high Cr content for the corrosion resistance of duplex stainless steel in batch digesters was demonstrated by Wensley[22]. Therefore, with higher alloying elements contents, S32750 behaved better corrosion resistance and higher strength than currently used S32205, and the use of S32750 in pulp and paper industry could prolong service life and reduce the thickness of facilities.

3.2 Potentiostatic polarization results

The potential -0.4 V_{SCE} was chosen to investigate the potentiostatic polarization behavior of S32750 in white liquor, as shown in Fig. 3. The current-time transients give the total current resulting from the formation and dissolution of passive film on S32750 in white liquor[23]. The current density initially decreases rapidly with time at all temperatures, which is attributed to the nucleation and growth of the passive films formed on S32750 at a rate higher than that of dissolution[24-26]. It can be observed that further increment of time results in a relatively steady state current density (i_{ss}), which is defined as the average value of current density recorded during the last 300 s. The value of i_{ss} increases with temperature indicating the decrease of protective ability of passive film on S32750. At 40 and 60 ^{0}C, the steady state of current densities is attributed to the formation of intact passive films on S32750. However, the significant current density fluctuations of current-time transients can be observed at 80 ^{0}C, which is related to either nucleation or metastable pitting events[27,28]. In addition, increasing temperature results in shortening the length of time before current density fluctuation, which means that the induction period of pits shortens and the corrosion process is accelerated at high temperature.

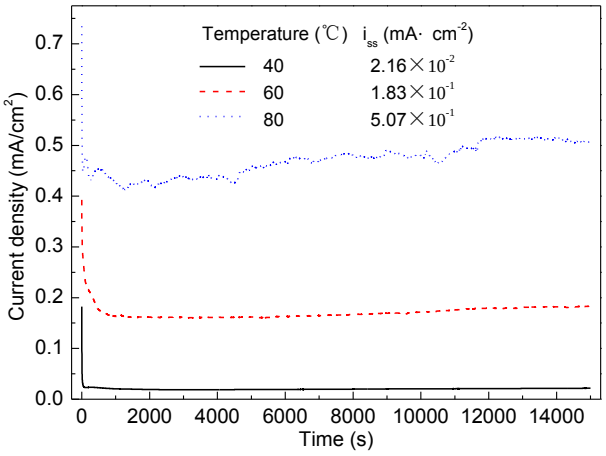

Figure 3. Potentiostatic polarization curve of S32750 in white liquor at different temperatures

The typical corrosion pit morphology was observed using SEM after potentiostatic polarization at 60 ^{0}C, as shown in Fig. 4(a). The pit occurs around the $MgO{\cdot}Al_2O_3$ composite inclusion analysed by the EDS, as shown in Fig. 4(b) and (c). For stainless steel, the location of the corrosion pits is associated with the inclusions and second phase precipitates[29,30]. Compared with other non-metallic inclusions, the MnS inclusion acting as preferential pit nucleation site is the most detrimental to corrosion resistance. Noh et al. suggested that MnS inclusions are preferred sites for pit initiation, especially when the sites are physically associated with another type of inclusion, such as oxide or silicate[31]. In the present research, pits around the $MgO{\cdot}Al_2O_3$ inclusion with a small amount of residual MnS ascribe to the preferential partial dissolution of MnS.

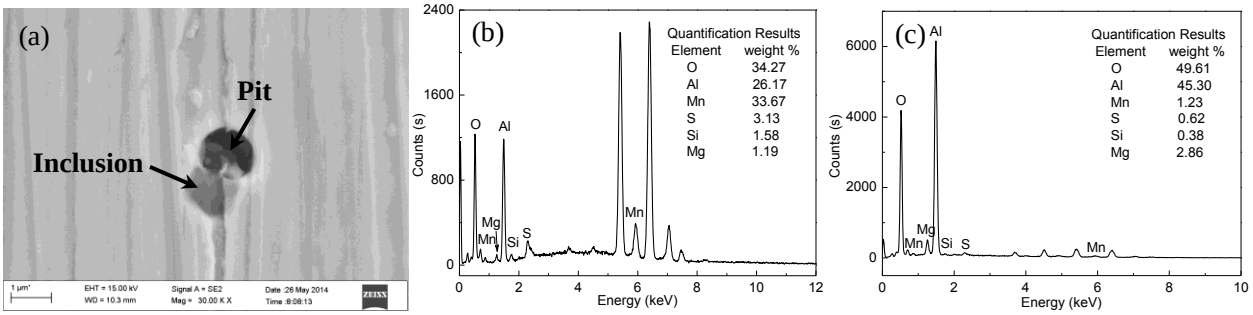

Figure 4. (a) Typical corrosion morphology and EDS analysis for (b) pit and (c) inclusion

3.3 EIS results

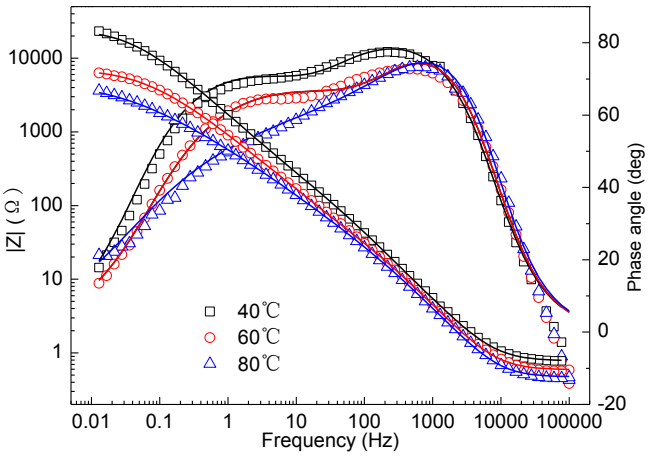

Figure 5. Bode plots of S32750 in white liquor at different temperatures

EIS tests were employed for better understanding the effect of temperature on the stability of the passive films formed on S32750 in white liquor. From bode plots shown in Fig. 5, it can be seen that impedance modulus values of all frequencies decrease with increasing temperature. It is reported that impedance modulus at high frequency represent the electrolyte resistance, and the solution viscosity of electrolyte reduces and diffusion rate of ions increases, which induces the decrease of electrolyte resistance[32]. Besides, the impedance modulus values at low frequency represent electrode

polarization resistance, which decreases with increasing temperature, revealing the deterioration of passive film and acceleration of corrosion rate. There exist two peaks in phase angle plot corresponding to two time constants, which indicates that the passive films formed on S32750 have bilayer structure[12]. And the phase angles are all lower than 90°, indicating a deviation from ideal capacitor behavior[33,34]. Therefore, the constant phase element (CPE) is necessary to account for the non-ideal behavior of the capacitive elements which is attributed to distribution of relaxation times resulting from surface heterogeneities, adsorption of species, and the formation of porous layers[35-37].

Baed on the bilayer structure of passive film in S32750, the equivalent circuit $R_s(Q_1(R_1(Q_2R_2)))$ was chosen to fit the EIS data. The equivalent circuit and structure of passive film is shown in Fig. 6, and the fitting parameters are listed in Table 3. In the circuits, R_s represents the electrolyte resistance, Q_1 and R_1 are the capacitance and resistance of the outer porous film, Q_2 and R_2 are the capacitance of the inner compact passive film (barrier film).

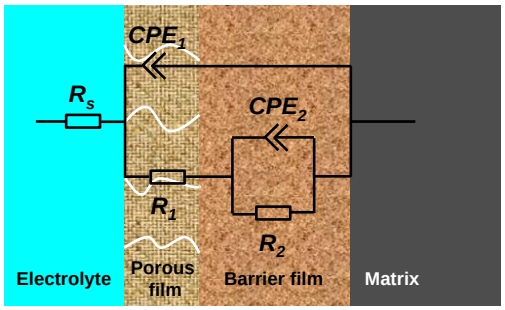

Figure 6. EIS equivalent circuit of S32750 in white liquor

Table 3. EIS equivalent circuit fitting results of S32750 in white liquor at different temperatures

Temperature (℃)	R_{sol} ($\Omega\cdot cm^{-2}$)	Q_1 ($\Omega^{-1}\cdot s^n\cdot cm^{-2}$)	n_1	R_1 ($\Omega\cdot cm^{-2}$)	Q_2 ($\Omega^{-1}\cdot s^n\cdot cm^{-2}$)	n_2	R_2 ($\Omega\cdot cm^{-2}$)
40	0.78	5.83×10^{-5}	0.92	384.7	7.38×10^{-5}	0.73	2.49×10^{4}
60	0.59	5.73×10^{-5}	0.95	52.4	2.18×10^{-4}	0.68	7.37×10^{3}
80	0.47	5.37×10^{-5}	0.96	26.0	5.00×10^{-4}	0.57	4.96×10^{3}

According to the fitting parameters shown in Table 3, R_1 and R_2 values decrease obviously with increasing temperature, indicating the decrease of protective ability of passive film. R_2 value of inner compact passive film (barrier film) is much larger than the R_1 of the outer porous film, indicating that the protective of passive film is predominantly attributed to the barrier film, which is consistent with other reports[38,39]. The capacitance data obtained from EIS can be used to estimate the passive film thickness by using Eq. (2), which is valid for the parallel plate capacitor model[40,41]:

$$C_0 = \frac{\varepsilon_0 \varepsilon A}{d_{ox}} \qquad (2)$$

where C_0 is the capacitance, ε_0 is the permittivity of vacuum (8.85×10^{-12} F/cm), ε is the relative dielectric constant of the layer, A is the effective area, and d_{ox} is the thickness of oxide layer. However, it is difficult to obtain an accurate thickness of the passive film, for the relative dielectric constant is not well established, although the value 15.6 has been used for passive film on stainless steel[42-44]. Nevertheless, the variation tendency of the passive film thickness can be obtained based on the capacitive response under different temperatures. Q_1 hardly changes with temperature, and Q_2 increases considerably with temperature, indicating that the inner layer becomes thinner.

The previous studies showed that sulphide addition to the caustic solution favors the formation of FeS, according to Eq. (3):[2,45]

$$HFeO_2^- + S^{2-} + 3H^+ = FeS + 2H_2O \quad (3)$$

However, FeS is generally nonadherent or may hydrolyze in water easily, which is mainly responsible for the formation of outer porous film. Similarly, a poorly-protective film formed on mild steel in sulphide-containing caustic solution, which was composed of iron oxide and iron sulphide.[46]

3.4 Mott-Schttky analysis

It is well known that the passive films formed on stainless steel exhibit semiconduction behavior[12,41,47], which can be described by the Mott-Schottky (M-S) analysis. In order to gain insight into the effect of temperature on electronic properties of the passive film formed on S32750 in white liquor, the M-S analysis was performed at different temperatures after the specimens were passivated at -0.4 V_{SCE} for 1 h. Based on M-S theory, the semiconducting properties can be determined by analyzing the interfacial capacitance as a function of the applied potential[27,42,48]. The interfacial capacitance C was calculated by the system software using Eq. (4).

$$\boldsymbol{C} = -\frac{1}{2\pi \boldsymbol{f} \boldsymbol{Z}''} \quad (4)$$

where $\boldsymbol{Z}''$ is the imaginary part of the impedance and f is the frequency.

The M-S relationship of n-type and p-type semiconductor is expressed by Eqs. (5) and (6), respectively.

$$\frac{1}{C^2} = \frac{2}{\varepsilon\varepsilon_0 q N_D}\left(E - E_{FB} - \frac{kT}{q}\right) \quad (5)$$

$$\frac{1}{C^2} = -\frac{2}{\varepsilon\varepsilon_0 q N_A}\left(E - E_{FB} - \frac{kT}{q}\right) \quad (6)$$

where q is the electron charge(1.602×10^{-19} C), N_D and N_A are the donor and acceptor densities, respectively. E_{FB} is the flat band potential, k is the Boltzmann constant (1.38×10^{-23} J/K), and T is the absolute temperature. N_D and N_A can be determined from the slope of the experimental $1/C^2$ vs. applied potential (E).

The M-S plots obtained for passivated S32750 in white liquor are shown in Fig. 7, which exhibit two liner regions. The negative slope of the straight line in region R1 indicates a p-type semiconductor for the passive film on S32750 was attributed to the enrichment of chromium in the inner layer. The positive slope of the straight line in region R2 indicates an n-type semiconductor,

which can be attributed to the outer porous iron-rich layer[38,49]. The interfacial capacitance increases with temperature significantly, revealing that the passive films become thinner[50], which is consistent with the results of potentiostatic polarization curves and EIS measurements.

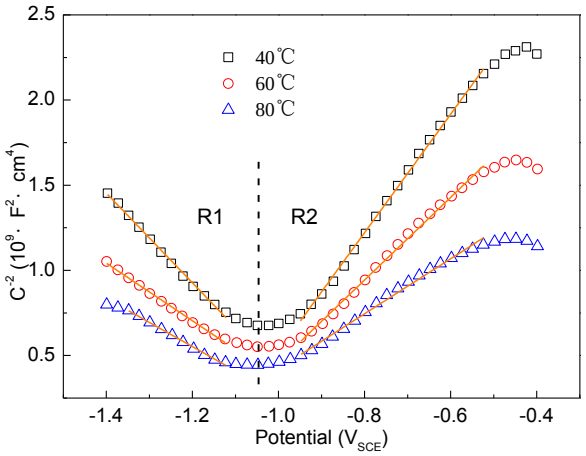

Figure 7. Mott-Schottky plots of S32750 in white liquor at different temperatures

The values of acceptor density (N_A) and donor density (N_D) corresponding to S32750 in white liquor are listed in Table 4, which are on the order of 10^{21} cm^{-3}, and agree well with the values obtained by other researchers[27,35]. High doping densities indicate the highly disordered character of passive films[42], which imply that the passive films formed on S32750 become more defective with increasing temperature. Meanwhile, it is reported that the N_A and N_D values are affected by conductivity of passive film, indicating that high acceptor or donor density with increasing temperature leads to high values of the passive current density, which are in agreement with the polarization curves.

Table 4. Acceptor and donor densities of passive film formed on S32750 in white liquor at different temperatures

Temperature(℃)	N_A (cm^{-3})	N_D(cm^{-3})
40	3.44×10^{21}	2.57×10^{21}
60	5.36×10^{21}	3.73×10^{21}
80	6.36×10^{21}	5.61×10^{21}

Furthermore, the thickness of space charge layer (W) of n-type semiconductor at applied potential can be calculated by Eq. (7)[15,51].

$$W = \left[\frac{2\varepsilon\varepsilon_0}{qN_D}\left(E - E_{FB} - \frac{kT}{q}\right)\right]^{1/2} \qquad (7)$$

The relationship between *W* and the applied potential for passive films formed on S32750 at -0.4 V_{SCE} for 1 h in white liquor in shown in Fig. 8. Since the space charge layer plays an effective barrier to the flow of carriers, such as electrons and holes, from semiconductor to electrolyte, the value of *W* decreases with increasing temperature reveals the decreasing of corrosion resistance[15,52].

Therefore, the increase of acceptor density, donor density and decrease of space charge layer thickness of passive films with increasing temperature indicating the passive films on S32750 in white liquor exhibit poor protective ability for corrosion resistance at high temperature.

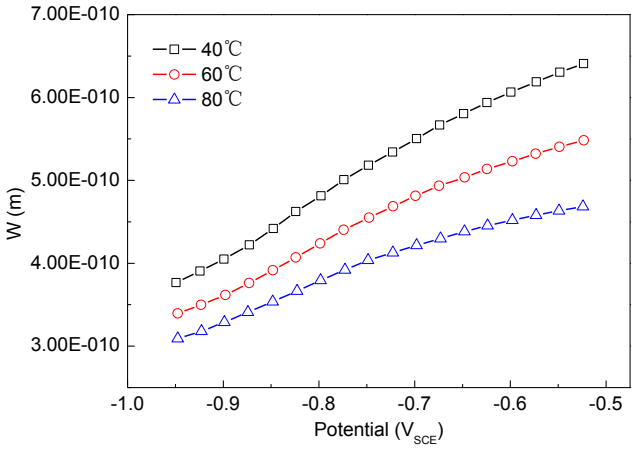

Figure 8. Relation between the space charge layer thickness and the applied potential of S32750 in white liquor at different temperatures

4. CONCLUSION

The effect of temperature on the corrosion behavior of super duplex stainless steel S32750 and comparison of corrosion resistance between S32750 and currently used S32205 in white liquor were investigated. The main conclusions are summarized as follows:

(1) The potentiodynamic polarization curves show the corrosion current density increases with temperature, indicating that the corrosion process is accelerated at higher temperatures. The corrosion potential of S32750 increases with temperature, which is different from S32205. The absence of active current peak or Flade potential of S32750 confirms the passive films previously formed in air kept passivity in white liquor, while S32205 behaved primary and secondary active-passive transition zones. Therefore, with better corrosion resistance and higher strength, application of S32750 would prolong service life and reduce the thickness of facilities.

(2) The potentiostatic polarization curves show the steady state current density increases, and the induction period of the pits is shortened with increasing temperature. These results indicate that the protective ability of the passive film decreases, and the corrosion process is accelerated. EDS shows that the pit occurred around the $MgO{\cdot}Al_2O_3$ composite inclusion with residual MnS, indicating the preferential partial dissolution of MnS.

(3) The EIS results reveal that the protection of the passive film is predominantly attributed to the barrier film. The polarization resistance of the passive film obviously decreases with increasing temperature, indicating the passive film becomes more porous and less protective at higher temperatures.

(4) The Mott-Schottky analysis shows that the passive film formed on S32750 in white liquor presents a bilayer structure, and behaves as n-type and p-type, respectively. The donor and acceptor densities increase and the space charge layer thickness decreases with increasing temperature. Therefore, the passive films become more defective, resulting in decreased protective abilities of the passive films.

ACKNOWLEDGEMENTS

The present research was financially supported by National Key Technology Research and Development Program of the Ministry of Science and Technology of China(No. 2012BAE04B01), High Technology Research and Development Program of China (No. 2015AA034301), National Natural Science Foundation of China(No.51304041), China Postdoctoral Science Foundation(No. 2013M530936) and Program for New Century Excellent Talents in University(No. N130502001).

Reference

1. A. Sharma, Sulaxna, A. K. Singh, *J. Mater. Environ. Sci.*, 3 (2012) 1009
2. A. Bhattacharya, P. M. Singh, *Corros. Sci*., 53 (2011) 71
3. P. M. Singh, O. Ige, J. Mahmood, *Corrosion*, 59(2003) 843
4. J. Ramo, O. Hyokyvirta, M. Sillanpaa, *Mater. Corros.*, 54 (2003) 37
5. I. Betova, M. Bojinov, O. Hyökyvirta, T. Saario, *Corros. Sci.*, 52 (2010) 1499
6. A. Wensley, presented at Corrosion 2000, Orlando, USA, 2000, paper no. 00589
7. www.outokumpu.com/SiteCollectionDocuments/Stainless_for_Pulp_Paper_Brochure.pdf
8. J. Nordstrom, B. Rung, presented at TAPPI Engineering Conference, Orlando, USA, 1993, p.1201
9. http://tools.outokumpu.com/spt/pub/upload/pubs_5293738.pdf
10. D. A. Wensley, R. S. Charlton, *Corrosion*, 36 (1980) 385
11. E. Blasco-Tamarit, A. Igual-Muñoz, J. García Antón, D. García-García, *Corros. Sci.*,50 (2008) 1848
12. M. V. Cardoso, S. T. Amaral, E. M. A. Martini, *Corros. Sci.*, 50 (2008) 2429
13. M. Gojic, D. Marijan, L. Kosec, *Corrosion*, 56 (2000) 839
14. H. Li, Z. Jiang, H. Feng, Q. Wang, W. Zhang, G. Fan, G. Li, L. Wang, *Int. J. Electrochem. Sci.*, 10 (2015) 1616
15. J. B. Lee, S. W. Kim, *Mater. Chem. Phys.*, 104 (2007) 98
16. X. Wei, J. H. Dong, J. Tong, Z. Zheng, W. Ke, *Int. J. Electrochem. Sci.*, 8(2013)887
17. D. H. Hur, Y. S. Park, *Corrosion*, 62 (2006) 745
18. C. Escriva-Cerdán, E. Blasco-Tamarit, D. M. García-García, J. García-Antón, A. Guenbour, *Corros. Sci.*, 56 (2012) 114
19. J. H. Wang, C. C. Su, Z. Szklarska-Smialowska, *Corrosion*, 40 (1988) 732
20. P. E. Manning, D. J. Duquette, *Corros. Sci.*, 20 (1980) 597
21. J. E. Truman, K. R. Pirt, in: R.A. Lula (Ed.), Duplex Stainless Steel, ASM, Metals Park, OH, USA, 1983, p. 113
22. A. Wensley, M. Moskal, W. Wilton, presented at Corrosion97, New Orleans, USA, 1997, paper no. 378

23. M. Lakatos-Varsányi, F. Falkenberg, I. Olefjord, *Electrochim. Acta*, 43 (1998) 187
24. R. M. Fernandez-Domene, E. Blasco-Tamarit, D. M. Garcia-Garcia, J. Garcia-Anton, *Corros. Sci.*, 52 (2010) 3453
25. J. Kim, S. Pyun, *Electrochim. Acta*, 40 (1995) 1863
26. J. J. Park, S. I. Pyun, W. J. Lee, H. P. Kim, *Corrosion*, 55 (1999) 380
27. Y. X. Qiao, Y. G. Zheng, W. Ke, P. C. Okafor, *Corros. Sci.*, 51 (2009) 979
28. G. O. Ilevbare, G. T. Burstein, *Corros. Sci.*, 43 (2001) 485
29. G. Wranglen, *Corros. Sci.*, 14 (1974) 331
30. R. Ke, R. Alkire, *J. Electrochem. Soc.*, 142 (1995) 4056
31. J. S. Noh, N. J. Laycock, W. Gao, D. B. Wells, *Corros. Sci.*, 42 (2000) 2069
32. C. F. Dong, H. Luo, K. Xiao, T. Sun, Q. Liu, X. G. Li, *J. WuHan. Univ. Technol.*, 26 (2011) 641
33. Y. Fu, X. Q. Wu, E.H. Han, W. Ke, K. Yang, Z.H. Jiang, *Electrochim. Acta*, 2009, 54(2009)1618
34. A. Carnot, I. Frateur, S. Zanna, B. Tribollet, I. Dubois-Brugger, P. Marcus, *Corros. Sci.*, 45 (2003) 2513
35. C. Escriva-Cerdan, E. Blasco-Tamarit, D. M. Garcia-Garcia, J. Garcia-Anton, R. Akid , J. Walton, *Electrochim. Acta.*, 111 (2013) 552
36. G. J. Brug, A. L. G. Vandeneeden, M. Sluytersrehbach, J. H. Sluyters, *J. Electroanal. Chem.*, 176 (1984) 275
37. F. B. Growcock, J. H. Jasinski, *J. Electrochem. Soc.*, 136 (1989) 2310
38. M. BenSalah, R. Sabot, E. Triki, L. Dhouibi, Ph. Refait, M. Jeannin, *Corros. Sci.*, 86 (2014) 61
39. M. Boudalia, A. Guenbour, A. Bellaouchou, R. M. Fernandez-Domene, J. Garcia-Anton, *Int. J. Corros.*, 2013 (2013) 1
40. D. Wallinder, J. Pan, C. Leygraf, A. Delblanc-Bauer, *Corros. Sci.*, 41 (1998) 275
41. D. D. Macdonald, A. Sun, N. Priyantha, P. Jayaweera, *J. Electroanal Chem.*, 572 (2004) 421
42. C. Escriva-Cerdan, E. Blasco-Tamarit, D.M. Garcia-Garcia, J. García-Antóna, A. Guenbour, *Electrochim. Acta*, 80 (2012) 248
43. H. He, T. Zhang, C. Zhao, K. Hou, *J. Appl. Electrochem.*, 39 (2009) 737
44. A. M. P. Simões, M. G. S. Ferreira, B. Rondot, M. da Cunha Belo, *J. Electrochem. Soc.*, 137 (1990) 82
45. G. Theus, R.W. Staehle, presented at Stress Corrosion Cracking and Hydrogen Embrittlement of Iron Base Alloys, Unieux-Firminy, France, 1973, p. 845
46. D. Tromans, *J. Electrochem. Soc.*, 127 (1980) 1253
47. R. S. Dutt, Jagannath, G. K. Dey, P. K. De, *Corros. Sci.*, 48 (2006) 2711
48. A. Di Paola, *Electrochim. Acta*, 34 (1989) 203
49. R. A. Antunes, M. C. L. de Oliveira, I. Costa, *Mater. Corros.*, 63 (2012) 586
50. Y. Fu, X.Q. Wu, E. H. Han, W. Ke, K. Yang, Z. H. Jiang, *J. Electrochem. Soc.*, 155 (2008) 455
51. J. Amri, T. Souier, B. Malki, B. Baroux, *Corros. Sci.*, 50 (2008) 431
52. H. B. Li, Z. H. Jiang, H. Feng, H. C. Zhu, B. H. Sun, Z. Li, *Int. J. Min. Met. Mater.*, 20 (2013) 850